

# Expanding the promiscuity of a natural-product glycosyltransferase by directed evolution

Gavin J Williams, Changsheng Zhang & Jon S Thorson

**Natural products, many of which are decorated with essential sugar residues, continue to serve as a key platform for drug development<sup>1</sup>. Adding or changing sugars attached to such natural products can improve the parent compound's pharmacological properties, specificity at multiple levels<sup>2</sup>, and/or even the molecular mechanism of action<sup>3</sup>. Though some natural-product glycosyltransferases (GTs) are sufficiently promiscuous for use in altering these glycosylation patterns, the stringent specificity of others remains a limiting factor in natural-product diversification and highlights a need for general GT engineering and evolution platforms. Herein we report the use of a simple high-throughput screen based on a fluorescent surrogate acceptor substrate to expand the promiscuity of a natural-product GT via directed evolution. Cumulatively, this study presents variant GTs for the glycorandomization of a range of therapeutically important acceptors, including aminocoumarins, flavonoids and macrolides, and a potential template for engineering other natural-product GTs.**

As an emerging method to differentially glycosylate natural products, glycorandomization uses the inherent or engineered substrate promiscuity of anomeric kinases (Fig. 1a, E<sub>1</sub>) and nucleotidyltransferases (E<sub>2</sub>) for the *in vitro* synthesis of sugar nucleotide libraries as sugar donors for natural-product GTs<sup>4</sup>. Although the successful glycorandomization of various natural-product scaffolds (including glycopeptides<sup>5</sup>, avermectins<sup>6</sup> and enediynes<sup>7</sup>) has been reported, other recent antibiotic glycorandomization attempts have revealed that aminocoumarin and macrolide GTs (NovM and EryBV, respectively) accept only 2 alternative sugar nucleotides out of 25 to 40 potential donors tested<sup>8,9</sup>. Thus, though permissive GTs open new opportunities for drug discovery, the stringent specificity of other GTs remains a limiting factor in natural-product diversification and highlights a need for general GT engineering and/or evolution platforms. Despite the wealth of GT structural and biochemical information<sup>10</sup>, attempts to alter GT donor/acceptor specificities via rational engineering have been largely unsuccessful and primarily limited to sequence-guided single-site mutagenesis<sup>11</sup>. Owing to a lack of high-throughput GT screens and selections, successful reports to alter GT donor/acceptor specificities via directed evolution are equally sparse. Although an

*in vivo* selection for the directed evolution of the sialyltransferase CstII (a unique member of the GT-A superfamily) was recently disclosed<sup>12</sup>, the directed evolution of any member of the structurally and functionally distinct GT-B superfamily has not been achieved.

One member of the GT-B superfamily<sup>13</sup>, the oleandomycin GT (OleD) from *Streptomyces antibioticus*, catalyzes the glucosylation of oleandomycin (**1**) using UDP-Glc (**2**) as donor to produce glucoside **3** (Fig. 1b)<sup>14</sup>. A recent mass spectrometry analysis of OleD specificity led to the identification of a range of small aromatic phenolics as putative OleD acceptors<sup>15</sup>. Notably, this panel included the fluorescent coumarin 4-methylumbelliferone (**4**) (Fig. 1b). Given the results of coumarin-based glycosynthase assays<sup>16</sup>, we postulated that **4** would offer the ability to directly assess OleD-catalyzed glycosyltransfer via fluorescence. Specifically, masking the C7 OH of **4** quenches fluorescence<sup>17</sup>. Preliminary rate determinations indicated the conversion rate of **4** to glucoside **5** (with **2** as donor using wild-type OleD) to be 300-fold less than the rate with the natural acceptor **1** (for example, Table 1 and Supplementary Fig. 1 online). Using the fluorescence-based assay, activity in *Escherichia coli* pET28/OleD crude cell extracts was reproducibly detected to be only ~two-fold higher than activity in cell extracts prepared from cultures that do not overexpress OleD (Fig. 2a). These preliminary studies confirmed **4** as a weak substrate for OleD. More importantly, these studies validated the fluorescence-based GT assay and set the stage to alter OleD catalytic efficiency and/or substrate promiscuity by directed evolution. A mutant OleD library was constructed by error-prone PCR using wild-type OleD as template, such that each variant had (on average) one or two amino acid mutations per gene product. A relatively small library (~1,000 colonies) of variants was initially screened using the fluorescence-based GT assay. For screening, extract aliquots were incubated with **4** and **2** and allowed to react for 3 h, after which the change in fluorescence intensity was measured.

Several potential positive hits were identified in the first round of screening (Fig. 2a), and three of these—designated 2C3, 7B9 and 8B3—were selected for further analysis. DNA sequencing of these hits revealed that 2C3 has a single amino acid mutation, A242V, whereas 7B9 and 8B3 each have two amino acid mutations, S132F/G340W and P67T/I112T, respectively. In order to assign functional mutations within 7B9 and 8B3, the corresponding four single mutants were constructed and characterized. A comparison of the specific activity of

Laboratory for Biosynthetic Chemistry, Pharmaceutical Sciences Division, School of Pharmacy, National Cooperative Drug Discovery Program, University of Wisconsin-Madison, 777 Highland Avenue, Madison, Wisconsin 53705, USA. Correspondence should be addressed to J.S.T. (jsthorson@pharmacy.wisc.edu).

Received 8 June; accepted 25 July; published online 9 September 2007; doi:10.1038/nchembio.2007.28

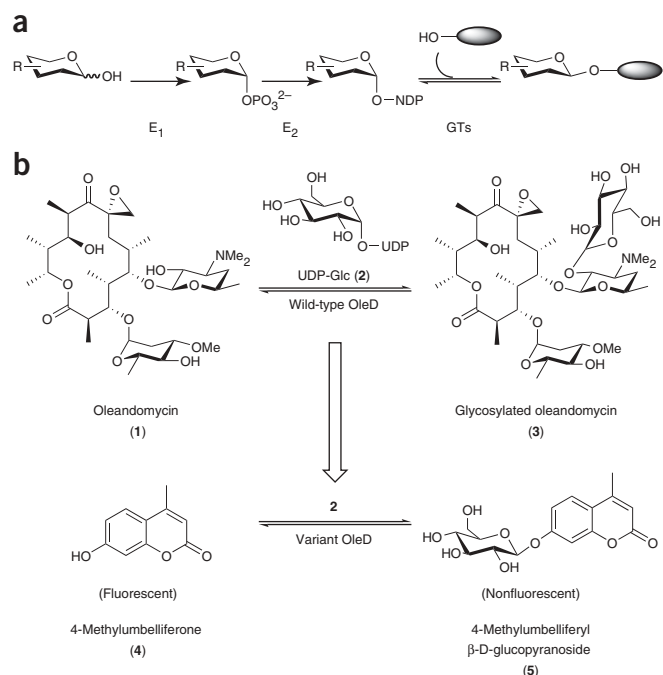


**Figure 1** Enzymatic glycosylation. (a) General overview of enzymatic glycorandomization.  $E_1$  represents a flexible anomeric sugar kinase,  $E_2$  represents a flexible sugar-1-phosphate nucleotidyltransferase, GTs represent a flexible glycosyltransferase and the gray oval represents a complex natural-product scaffold. (b) The native macrolide glucosyltransferase reaction catalyzed by OleD (upper reaction), and the 4-methylumbelliferone (**4**) glucosylation reaction used for OleD directed evolution (lower reaction).

the wild-type and mutant OleDs using the substrate pair **4** and **2** confirmed the first-generation variants 2C3, 7B9 and 8B3 to be more active than wild-type OleD (Fig. 2b) and revealed that the G340W (from 7B9) and I112T (from 8B3) mutations are each nonfunctional.

The remaining three functional mutations were subsequently combined by site-directed mutagenesis to provide the mutant P67T/S132F/A242V, the specific activity of which was determined to be  $\sim 30$ -fold higher than that of wild-type OleD with **4** and **2** as acceptor and donor, respectively.

The wild-type and triple-mutant OleD were compared by determining steady state kinetic parameters with **4** or **2** as variable substrates, as described in the **Supplementary Methods** online. The wild-type enzyme could not be saturated with **4** (**Supplementary Fig. 2** online), even at the solubility limit of **4** in water/DMSO (10 mM), which indicates that **4** is a poor substrate for wild-type OleD. Nevertheless, a  $k_{\text{cat}}/K_m$  value of  $0.18 \text{ mM}^{-1} \text{ min}^{-1}$  was determined by linear regression. Saturation was observed by varying donor **2** at a fixed concentration of **4** (10 mM) to provide an apparent  $K_m$  of 0.3 mM. However, the  $V_{\text{max}}$  from this analysis is unlikely to represent the true  $k_{\text{cat}}$ . The steady state kinetics of the triple-mutant P67T/S132F/A242V were very different from those of the wild-type enzyme. Saturation with **4** could be achieved to give an apparent  $K_m$  of 0.14 mM and a  $k_{\text{cat}}$  of  $1.48 \text{ min}^{-1}$  (**Supplementary Fig. 2**). An apparent donor  $K_m$  of 0.03 mM (a ten-fold improvement over

**Table 1** Wild-type and mutant OleD glucosylation rates with acceptors **1**, **4** and **27–32**

Acceptor	Enzyme					Fold improvement <sup>a</sup>
	WT	P67T	S132F	A242V	P67T/S132F/A242V	
Oleandomycin ( <b>1</b> )	700	200	1,487	70	13	0.02
4-Methylumbelliferone ( <b>4</b> )	2.5	15.7	6.3	5.4	84	33
7-Hydroxycoumarin-4-acetic acid ( <b>27</b> )	ND <sup>b</sup>	0.22	0.08	0.16	3.6	>180
7-Hydroxycoumarin-3-carboxylic acid ( <b>28</b> )	0.01	0.022	0.022	0.01	0.62	62
Novobiocic acid ( <b>29</b> )	0.24	0.65	0.49	0.33	1.14	4.8
Kaempferol ( <b>30</b> )	13.2	99.9	23	15.3	28	2.1
Daidzein ( <b>31</b> )	4.2	16.0	5.5	8.5	24	5.7
Genistein ( <b>32</b> )	3.4	28.8	8.8	14.1	26	7.7

Rates of glucoside formation are shown in nanomoles of product formed per minute per mg of enzyme. See Methods for assay conditions and detection details.

<sup>a</sup>Fold improvement of P67T/S132F/A242V compared with wild-type OleD. For glucosyltransfer to **1**, standard error of the assay is  $\pm 12\%$  of the rate. For transfer to **4** or **27**, **28**, **29**, **30**, **31**, **32**, standard error is less than 10%. <sup>b</sup>ND, not detected ( $< 0.01$  nanomoles of product formed per minute per mg of enzyme). See **Figure 1** for structures of acceptors **1** and **4**.

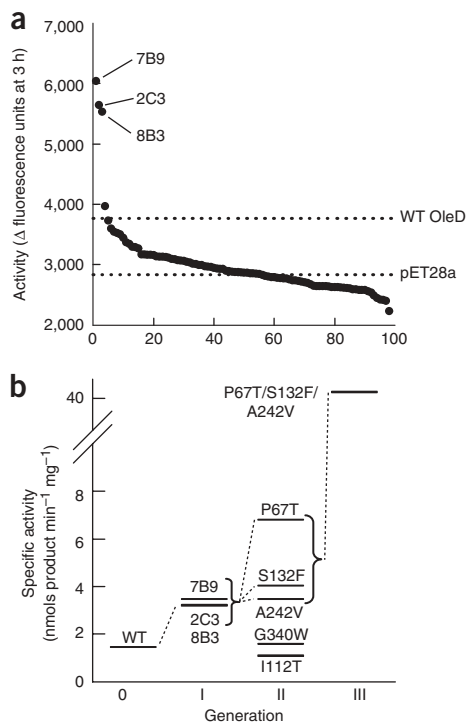


**Figure 2** Outcome of OleD directed evolution. **(a)** Representative screening data for the glycosylation of fluorescent **4** illustrating  $\sim 100$  random members from a mutant OleD library and the positive hits 2C3, 7B9 and 8B3. **(b)** Progression of GT activity toward **4**. Clone 2C3 had a single amino acid change (A242V), whereas clones 7B9 and 8B3 each had two mutations (S132F/G340W and P67T/I112T, respectively). WT, wild-type.

wild-type OleD) was determined using a fixed concentration of **4** and varying the concentration of **2**. Moreover, the triple-mutant  $k_{\text{cat}}$  values determined with either donor **2** or acceptor **4** as the variable substrate were in good agreement. Thus, in the context of **4** glycosylation, the triple mutant was  $\sim 60$ -fold more efficient than wild-type OleD.

Variant enzymes identified via directed evolution are often found to be promiscuous toward substrates well beyond those originally screened against<sup>18</sup>. To assess the impact of directed evolution on sugar nucleotide donor promiscuity, wild-type OleD and the P67T/S132F/A242V mutant were probed using a simple end-point assay with a library of 20 potential ‘unnatural’ UDP donors (**6–26**) as well as UDP-Glc and dTDP-Glc in the presence of **4** as the acceptor (Fig. 3a). This library included both commercially available sugar nucleotides (**2**, **6** and **10**) and unnatural sugar nucleotides generated via chemoenzymatic synthesis, cumulatively representing alterations of the sugar at C’1, C’2, C’3, C’4 or C’6. The product identities were confirmed by LC-MS and coelution with commercial standards where available (Supplementary Table 1 online). Of the 22 sugar nucleotides tested, only UDP-Glc (**2**), UDP-6-deoxyglucose (**8**) and UDP-6-thioglucose (**9**) led to detectable product with wild-type OleD, ranging from 1% to 14% conversion in 3 h (Fig. 3b and Supplementary Table 1). Thus, with the exception of very limited tolerance to C’6 modification, wild-type OleD showed stringent sugar donor specificity. In contrast, the evolved triple mutant P67T/S132F/A242V accepted 15 of 22 sugar nucleotide donors examined, 12 of which were not detectable substrates of wild-type OleD, with synthetic improvements ranging from 7- to 300-fold. Notably, tolerance to the sugar C’6 modification was most enhanced to allow new

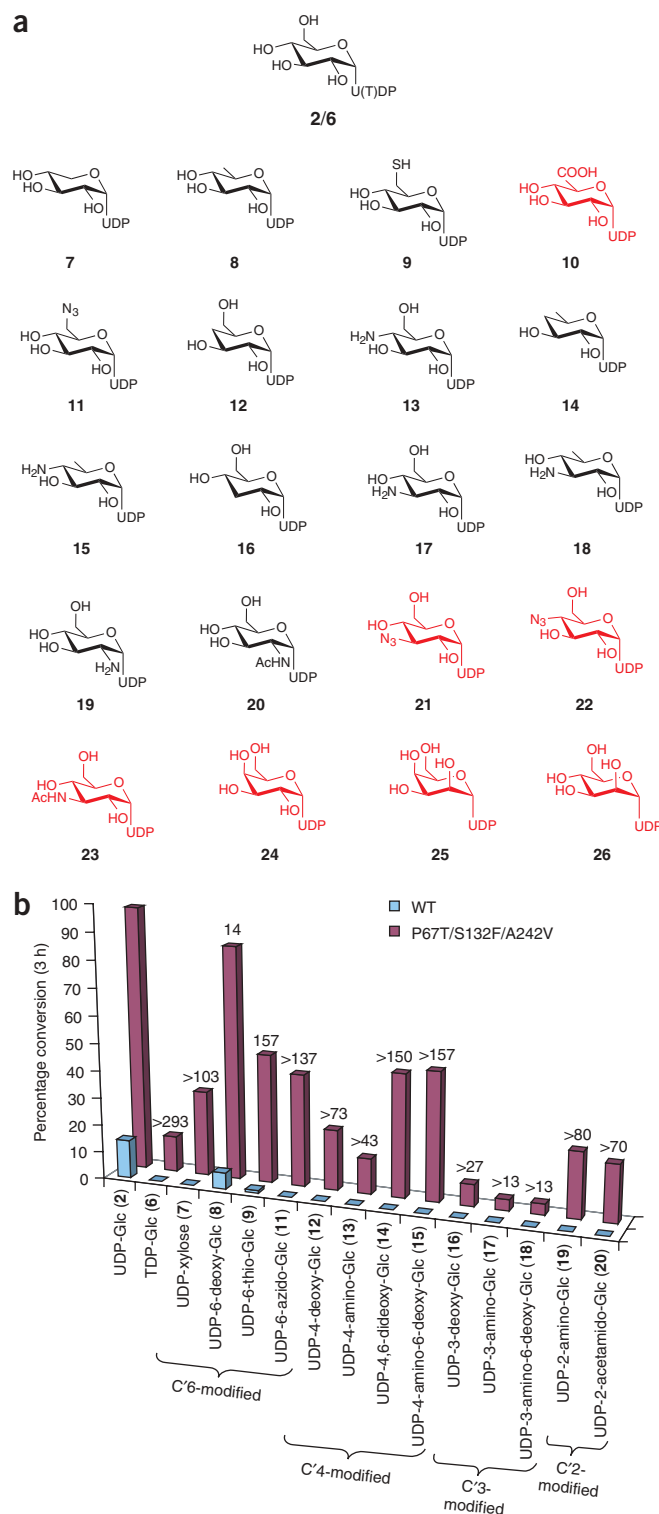
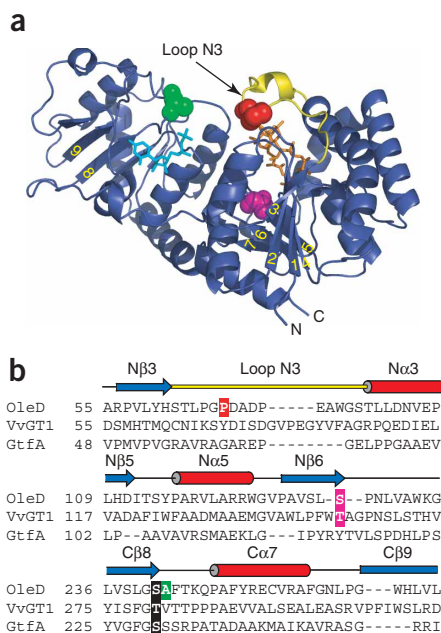


**Figure 3** Activity of wild-type OleD and variant P67T/A242V/S132F toward a set of NDP-sugar donors. **(a)** Structures of the donors tested. NDP-sugar donors that were not detectable substrates for either enzyme are shown in red. **(b)** Conversion rates of wild-type OleD and P67T/A242V/S132F toward each donor with **4** as acceptor. Donors that did not show activity with either enzyme were omitted for clarity (**10**, **21–26**). Numbers above bars indicate fold improvement from wild-type OleD, using an estimated minimal detection limit of 0.3% conversion for **4**. See Supplementary Methods for assay conditions and detection method.



C'-modified glycosides, including analogs (UDP-6-thiogluco-**9**) and UDP-6-azidogluco-**11**) that present the potential for further downstream chemoselective diversification<sup>5</sup>.

To estimate the impact of each individual mutation on donor specificity, a subset of six donors was used to probe the specificity of the single mutants P67T, S132F and A242V (**Supplementary Table 2** online) with **4** as the acceptor in an identical end-point assay. This subset consisted of the natural donor UDP-Glc (**2**), UDP-xylose (**7**), and the 6-deoxy (**8**), 6-azido (**11**), 4-deoxy (**12**) and 2-amino (**19**) derivatives. Notably, all single mutants led to  $\leq 2\%$  conversion with donor analogs **7**, **11**, **12** and **19**, and they all led to poor conversion ( $\leq 12\%$ ) with **8**. Thus, the improved donor range of the triple mutant likely derives from the synergistic combination of P67T, S132F and A242V. The same donor subset using **1** as acceptor and triple mutant P67T/S132F/A242V as the catalyst led to the desired product in nearly quantitative yield in every case (**Supplementary Fig. 3** online). Given the role of differential glycosylation in modulating the biological effects of macrolides—including bacterial ribosome 50S ribosome inhibition<sup>19</sup>, immunomodulation<sup>20</sup>, and inhibition of Golgi transport<sup>21</sup>—this preliminary study is an advance toward the synthesis of such analogs.

Given the ability of wild-type OleD to glycosylate a range of small phenolics<sup>15</sup>, we examined the acceptor specificity of the wild-type and mutant OleDs by measuring the rate of glucoside formation using a panel of six additional acceptors (**27–32**; **Table 1**), including the natural macrolide substrate **1**. In each case, the appearance of a major new product peak was monitored over a suitable time interval during which the rate of formation was linear. The products were identified by LC-MS, comparison to commercial standards where available, and fluorescence measurements (**Supplementary Figs. 4** and **5** online). Compared with the natural substrate **1**, wild-type OleD showed a 50- to 500-fold lower activity with screening target **4**, flavonoid **30** and isoflavones **31** and **32**, whereas the charged coumarins **27** and **28** were essentially nondetectable substrates for wild-type OleD. However, aminocoumarin **29** was accepted by the wild-type enzyme, albeit at a rate  $\sim 3,000$ -fold less than with **1**. Once again in stark contrast, the mutant P67T/S132F/A242V activity toward the

**Figure 4** Location of functional amino acid mutations. **(a)** Crystal structure of OleD (PDB ID 21YF) highlighting the locations of functional amino acid mutations as colored spheres: Pro67, red; Ser132, magenta; Ala242, green. Loop N3 is shown in yellow, UDP and non-natural acceptor erythromycin are shown in cyan and orange, respectively, and  $\beta$ -strands, where visible, are numbered sequentially. **(b)** Sequence alignment of OleD (Entrez Protein accession code ABA42119), the plant GT VvGT1 (Entrez Protein accession code AAB81683), and Gt fA (Entrez Protein accession code AAB49292). Secondary structure of OleD is shown above the OleD sequence.  $\beta$ -sheets, blue;  $\alpha$ -helices, red; loop N3, yellow. OleD Pro67 is highlighted red, OleD/VvGT1 Ser132/Thr141 are highlighted magenta, OleD Ala242 is highlighted green, and the conserved serine/threonine that likely interacts with  $\alpha$ -phosphate of the donor is highlighted black.

entire panel of small phenolics (**4** and **27–32**) was improved compared with wild-type OleD. Surprisingly, the largest improvement in activity was not observed with the screening target **4**; instead, it was observed with 7-hydroxycoumarin-4-acetic acid (**27**). In addition to their well-known antioxidant activities, glycosylated coumarins and flavonoids have diverse biological activities including anticancer<sup>22</sup>, antiangiogenesis<sup>23</sup>, anti-HIV<sup>24</sup> and anti-inflammatory<sup>25</sup> effects. The modest improvement toward aminocoumarin **29** is also notable, particularly in the context of the observed donor promiscuity of P67T/S132F/A242V, as the antibiotic novobiocin (**33**) (a glycosylated version of **29**) is an established inhibitor of DNA gyrase and induces degradation of Hsp90-dependent client proteins<sup>26</sup>. Concomitant with the enhancement of activity toward small aromatic acceptors, the evolved triple mutant glucosylated the natural acceptor **1** at a rate  $\sim 54$ -fold less than that of the wild-type enzyme. However, the single mutant S132F was  $\sim 2$ -fold more active toward **1** than wild-type OleD. Apart from this difference, the single mutants P67T, S132F and A242V were less active than the triple mutant toward all the acceptors tested; the P67T mutation was clearly the most advantageous single functional mutation.

The recently determined structure of OleD allows structural interpretation for the functional effects of the mutations discovered in this study<sup>13</sup>. The most advantageous single functional mutation at Pro67 is present in a loop region (amino acids 60–76, loop N3) that contains several prolines and follows  $\beta$ -sheet 3 in the N-terminal domain (**Fig. 4**). This loop is hypervariable in other GT-B fold GTs and constitutes part of the acceptor binding site<sup>27</sup>. For example, the loop immediately following N $\beta$ 3 in Gt fA (residues 57–72, **Fig. 4b**) forms a broad binding surface containing two prolines at positions 68 and 69 (ref. 28). Coincidentally, this loop has been interrogated by mutation in at least one other reported example aimed at identifying the residues responsible for donor selectivity in the urdamycin GTs. In the previous UrdGT mutagenesis study, sequence alignments were used to guide the construction of a series of defined hybrid and residue-exchanged UrdGT1b and UrdGT1c enzymes, the activities of which were assayed using a low-throughput HPLC assay<sup>29</sup>. Consequently, a 31-amino-acid region (residues 52–82) was determined to be responsible for donor specificity, and mutation at a single position equivalent to a proline (Pro56) within this region was found to be sufficient to alter UrdGT specificity<sup>30</sup>. In conjunction with the present OleD directed evolution study, this previous GT mutagenesis study highlights the importance of key prolines within the GT-B loop N3, which may (in part) define GT-B acceptor specificity.

Ser132 is also closely associated with the active site of OleD, which is located at the N terminus of  $\beta$ -strand 5 in the N-terminal domain of OleD (**Fig. 4a**). This residue is partially conserved as serine, threonine or alanine in related natural-product GTs. Comparison to the sequence and structure of the plant flavonoid GT-B fold enzyme

VvGT1 (ref. 31) reveals a likely role for Ser132 in binding the donor sugar. The VvGT1 equivalent to the OleD Ser132 (Thr141) forms a hydrogen bond with the C6 OH of UDP-2-deoxy-2-fluoroglucose. Thus, mutation of Ser132 in OleD may alter binding of the donor. Similarly, Ala242 is partially conserved as alanine, serine or threonine in related GTs. In the OleD structure, Ala242 follows Ser241, which forms a hydrogen bond to the  $\alpha$ -phosphate of the donor—an interaction that is also observed in the VvGT1 structure. Mutation of Ala242 may therefore affect binding of the diphosphate moiety of the UDP donor or in turn alter binding of the sugar moiety.

In an effort to overcome the limited substrate specificity of a natural-product GT, we have used directed evolution to improve the promiscuity of the macrolide GT OleD. Aside from the considerable expansion of both donor and acceptor specificity of the evolved enzyme, a number of additional key elements of this study are of importance. First, this work illustrates the ability to substantially alter GT specificity and proficiency via a single (or a few combined) mutation and thereby provides promise for future GT engineering efforts where assay design may limit throughput. Second, this study lends support to the observation that an increase in enzyme proficiency leads to an increase in promiscuity<sup>32</sup>, and it also reveals the potential to create promiscuous variants of other natural-product GTs simply by screening for efficiency toward a single acceptor-donor pair. Third, this study exposes the GT-B fold loop N3 as a potential focal point for future GT engineering efforts and, in the context of OleD, presents a new scaffold for further rational redesign or directed evolution. Finally, given that many of the acceptors for the newly evolved GT are therapeutically relevant (for example, macrolides, flavonoids, isoflavones, aminocoumarins and coumarins), this broadly promiscuous ‘universal’ GT presents opportunities in drug discovery and will also enhance ongoing efforts to develop bacterial hosts for *in vivo* glycorandomization<sup>33</sup>.

## METHODS

**General.** Bacterial strain *E. coli* BL21(DE3)pLysS was purchased from Stratagene. NovaBlue was purchased from Novagen. Plasmid pET28/OleD was a gift (see Acknowledgments), and pET28a was purchased from Novagen. All other chemicals were reagent-grade and purchased from Fluka, New England Biolabs or Sigma, unless otherwise stated. Primers were ordered from Integrated DNA Technologies. Oleandomycin was purchased from MP Biomedicals Inc. Phenolic substrates (27, 28, 30, 31, 32) were from Indofine Chemical Company Inc. Novobiocin (29) was prepared as previously described from Novobiocin (33)<sup>8</sup>. Product standard 4-methylumbelliferyl-7-O- $\beta$ -D-glucoside (5) was purchased from Sigma, and daidzein-7-O- $\beta$ -D-glucoside (34) standard was purchased from Fluka. Analytical HPLC was performed on a Rainin Dynamax SD-2/410 system connected to a Rainin Dynamax UV-DII absorbance detector. Mass spectra were obtained using electrospray ionization on an Agilent 1100 HPLC-MSD SL quadrupole mass spectrometer connected to a UV-Vis diode array detector. For LC-MS analysis, quenched reaction mixtures were analyzed by analytical reverse-phase HPLC with a 250 mm  $\times$  4.6 mm Gemini 5 $\mu$  C18 column (Phenomenex), using a gradient of 10–90% CH<sub>3</sub>CN in 0.1% formic acid/H<sub>2</sub>O for 20 min at 1 ml min<sup>-1</sup>, with detection at 254 nm.

**Library preparation.** The random mutant library was prepared via error-prone PCR using the Stratagene GeneMorph II Random Mutagenesis Kit, as described by the manufacturer with pET28/OleD as template. The primers used for amplification of the OleD gene were T7 FOR (5'-TAA TAC GAC TCA CTA TAG GG-3') and T7 REV (5'-GCT AGT TAT TGC TCA GCG G-3'). Amplified product was digested with *Nde*I and *Hind*III, purified by agarose gel electrophoresis (0.8% w/v agarose), extracted using the QIAquick Gel Extraction Kit (QIAGEN), and ligated into similarly treated pET28a. The ligation mixtures were used to transform chemically competent NovaBlue cells and single colonies

used to prepare plasmids for DNA sequencing, which revealed that the library had the desired mutation rate of 1 or 2 amino acid mutations per gene product. Subsequently, all the transformants from this library were pooled and cultured overnight. Plasmids were prepared from this culture and used to transform chemically competent *E. coli* BL21(DE3)pLysS, which was screened as described below.

**Site-directed mutagenesis.** Site-specific OleD variants were constructed using the Stratagene QuikChange II Site-Directed Mutagenesis Kit, as described by the manufacturer. Constructs were confirmed to carry the correct mutations via DNA sequencing.

**Screening.** Individual colonies were used to inoculate wells of a 96-deep-well microtiter plate in which each well contained 1 ml of LB medium supplemented with 50  $\mu$ g ml<sup>-1</sup> kanamycin. Culture plates were tightly sealed with AeraSea breathable film (Research Products International Corp.). After cell growth at 37 °C for 18 h with shaking at 350 r.p.m., 100  $\mu$ l of each culture was transferred to a fresh deep-well plate containing 1 ml of LB medium supplemented with 50  $\mu$ g ml<sup>-1</sup> kanamycin. The original plate was sealed and stored at 4 °C, or a glycerol copy was made by mixing 100  $\mu$ l of each culture with 100  $\mu$ l of 50% (v/v) glycerol and stored at -80 °C. The freshly inoculated plate was incubated at 37 °C for 2–3 h with shaking at 350 r.p.m. Expression of the N-terminal His<sub>6</sub>-tagged OleD was induced at an optical density at 600 nm (OD<sub>600</sub>) of ~0.7 via the addition of IPTG to a final concentration of 0.4 mM, and the plate was incubated for 18 h at 18 °C. Cells were harvested by centrifugation at 3,000g for 10 min at 4 °C, the cell pellets were thoroughly resuspended in 50 mM Tris-HCl (pH 8.0) containing 10  $\mu$ g ml<sup>-1</sup> lysozyme (Sigma) at 4 °C, and the plates were subjected to a single freeze-thaw cycle to lyse the cells. Cell debris was then collected by centrifugation at 3,000g for 20 min at 4 °C, and 50  $\mu$ l of the cleared supernatant was used for enzyme assay.

For the assay, cleared supernatant was mixed with an equal volume (50  $\mu$ l) of 50 mM Tris-HCl (pH 8.0) containing 10 mM MgCl<sub>2</sub>, 0.2 mM 4 and 1.0 mM 2 using a Biomek FX Liquid Handling Workstation (Beckman Coulter). Upon mixing, the initial fluorescence ( $\lambda_{\text{ex}} = 350$  nm,  $\lambda_{\text{em}} = 460$  nm) was measured using a FLUOstar Optima plate reader (BMG Labtechnologies). The reactions were subsequently incubated for 3 h at 30 °C, at which time the fluorescence measurement was repeated. Activity of the clones was expressed as the difference in fluorescence intensity between 0 h and 3 h.

**Other methods.** For all other methods, including probing acceptor/donor specificity, sugar nucleotide synthesis, and determination of kinetic parameters, see **Supplementary Methods**.

**Accession codes.** Protein Data Bank: The OleD crystal structure can be found as PDB ID 2IYF. Entrez Protein: the sequence alignment of OleD can be found under accession code ABA42119, the sequence of plant GT VvGT1 is under accession code AAB81683, and the sequence of GtfA is under accession code AAB49292. All sequences were deposited as part of previous studies.

*Note: Supplementary information and chemical compound information is available on the Nature Chemical Biology website.*

## ACKNOWLEDGMENTS

We are grateful to the School of Pharmacy Analytical Instrumentation Center for analytical support, H.-W. Liu (University of Texas-Austin) for plasmid pET28/OleD and S. Singh for helpful discussions. This work was supported in part by the US National Institutes of Health grants AI52218 and U19 CA113297. J.S.T. is a University of Wisconsin H.I. Romnes Fellow.

## AUTHOR CONTRIBUTIONS

G.J.W. contributed to the experimental design, experimental execution and manuscript drafting; C.Z. contributed experimental reagents and consultation; and J.S.T. contributed to the experimental design and manuscript drafting.

## COMPETING INTERESTS STATEMENT

The authors declare competing financial interests: details accompany the full-text HTML version of the paper at <http://www.nature.com/naturechemicalbiology/>.

Published online at <http://www.nature.com/naturechemicalbiology>  
 Reprints and permissions information is available online at <http://npg.nature.com/reprintsandpermissions>

- Weymouth-Wilson, A.C. The role of carbohydrates in biologically active natural products. *Nat. Prod. Rep.* **14**, 99–110 (1997).
- Thorson, J.S. & Vogt, T. in *Carbohydrate-Based Drug Discovery* (ed. Wong, C.-H.) 685–712 (Wiley-VCH, Weinheim, Germany, 2002).
- Ahmed, A. *et al.* Colchicine glycorandomization influences cytotoxicity and mechanism of action. *J. Am. Chem. Soc.* **128**, 14224–14225 (2006).
- Griffith, B.R., Langenhan, J.M. & Thorson, J.S. 'Sweetening' natural products via glycorandomization. *Curr. Opin. Biotechnol.* **16**, 622–630 (2005).
- Fu, X. *et al.* Antibiotic optimization via *in vitro* glycorandomization. *Nat. Biotechnol.* **21**, 1467–1469 (2003).
- Zhang, C., Albermann, C., Fu, X. & Thorson, J.S. The *in vitro* characterization of the iterative avermectin glycosyltransferase AveBI reveals reaction reversibility and sugar nucleotide flexibility. *J. Am. Chem. Soc.* **128**, 16420–16421 (2006).
- Zhang, C. *et al.* Exploiting the reversibility of natural product glycosyltransferase-catalyzed reactions. *Science* **313**, 1291–1294 (2006).
- Albermann, C. *et al.* Substrate specificity of NovM: implications for novobiocin biosynthesis and glycorandomization. *Org. Lett.* **5**, 933–936 (2003).
- Zhang, C., Fu, Q., Albermann, C., Li, L. & Thorson, J.S. The *in vitro* characterization of the erythronolide mycarosyltransferase EryBV and its utility in macrolide diversification. *ChemBioChem* **8**, 385–390 (2007).
- Hu, Y. & Walker, S. Remarkable structural similarities between diverse glycosyltransferases. *Chem. Biol.* **9**, 1287–1296 (2002).
- Hancock, S.M., Vaughan, M.D. & Withers, S.G. Engineering of glycosidases and glycosyltransferases. *Curr. Opin. Chem. Biol.* **10**, 509–519 (2006).
- Aharoni, A. *et al.* High-throughput screening methodology for the directed evolution of glycosyltransferases. *Nat. Methods* **3**, 609–614 (2006).
- Bolam, D.N. *et al.* The crystal structure of two macrolide glycosyltransferases provides a blueprint for host cell antibiotic immunity. *Proc. Natl. Acad. Sci. USA* **104**, 5336–5341 (2007).
- Quiros, L.M., Aguirrezabalaga, I., Olano, C., Mendez, C. & Salas, J.A. Two glycosyltransferases and a glycosidase are involved in oleandomycin modification during its biosynthesis by *Streptomyces antibioticus*. *Mol. Microbiol.* **28**, 1177–1185 (1998).
- Yang, M. *et al.* Probing the breadth of macrolide glycosyltransferases: *in vitro* remodeling of a polyketide antibiotic creates active bacterial uptake and enhances potency. *J. Am. Chem. Soc.* **127**, 9336–9337 (2005).
- Mayer, C. *et al.* Directed evolution of new glycosynthases from *Agrobacterium* beta-glucosidase: a general screen to detect enzymes for oligosaccharide synthesis. *Chem. Biol.* **8**, 437–443 (2001).
- Collier, A.C., Tingle, M.D., Keelan, J.A., Paxton, J.W. & Mitchell, M.D. A highly sensitive fluorescent microplate method for the determination of UDP-glucuronosyl transferase activity in tissues and placental cell lines. *Drug Metab. Dispos.* **28**, 1184–1186 (2000).
- Carr, R. *et al.* Directed evolution of an amine oxidase possessing both broad substrate specificity and high enantioselectivity. *Angew. Chem. Int. Edn Engl.* **42**, 4807–4810 (2003).
- Katz, L. & Ashley, G.W. Translation and protein synthesis: macrolides. *Chem. Rev.* **105**, 499–528 (2005).
- Amsden, G.W. Anti-inflammatory effects of macrolides—an underappreciated benefit in the treatment of community-acquired respiratory tract infections and chronic inflammatory pulmonary conditions. *J. Antimicrob. Chemother.* **55**, 10–21 (2005).
- Bonay, P., Munro, S., Fresno, M. & Alarcon, B. Intra-Golgi transport inhibition by megalomicin. *J. Biol. Chem.* **271**, 3719–3726 (1996).
- Lacy, A. & O'Kennedy, R. Studies on coumarins and coumarin-related compounds to determine their therapeutic role in the treatment of cancer. *Curr. Pharm. Des.* **10**, 3797–3811 (2004).
- Yuan, H.Q., Junker, B., Helquist, P. & Taylor, R.E. Synthesis of anti-angiogenic isocoumarins. *Curr. Org. Synth.* **1**, 1–9 (2004).
- Williams, C.A. & Grayer, R.J. Anthocyanins and other flavonoids. *Nat. Prod. Rep.* **21**, 539–573 (2004).
- Fylaktakidou, K.C., Hadjipavlou-Litina, D.J., Litinas, K.E. & Nicolaides, D.N. Natural and synthetic coumarin derivatives with anti-inflammatory/antioxidant activities. *Curr. Pharm. Des.* **10**, 3813–3833 (2004).
- Burlison, J.A., Neckers, L., Smith, A.B., Maxwell, A. & Blagg, B.S. Novobiocin: redesigning a DNA gyrase inhibitor for selective inhibition of Hsp90. *J. Am. Chem. Soc.* **128**, 15529–15536 (2006).
- Mulichak, A.M., Lu, W., Losey, H.C., Walsh, C.T. & Garavito, R.M. Crystal structure of vancosaminyltransferase GtfD from the vancomycin biosynthetic pathway: interactions with acceptor and nucleotide ligands. *Biochemistry* **43**, 5170–5180 (2004).
- Mulichak, A.M. *et al.* Structure of the TDP-epi-vancosaminyltransferase GtfA from the chloroeremomycin biosynthetic pathway. *Proc. Natl. Acad. Sci. USA* **100**, 9238–9243 (2003).
- Hoffmeister, D., Ichinose, K. & Bechthold, A. Two sequence elements of glycosyltransferases involved in urdamycin biosynthesis are responsible for substrate specificity and enzymatic activity. *Chem. Biol.* **8**, 557–567 (2001).
- Hoffmeister, D. *et al.* Engineered urdamycin glycosyltransferases are broadened and altered in substrate specificity. *Chem. Biol.* **9**, 287–295 (2002).
- Offen, W. *et al.* Structure of a flavonoid glucosyltransferase reveals the basis for plant natural product modification. *EMBO J.* **25**, 1396–1405 (2006).
- Oberthür, M. *et al.* A systematic investigation of the synthetic utility of glycopeptide glycosyltransferases. *J. Am. Chem. Soc.* **127**, 10747–10752 (2005).
- Hui, J.P., Yang, J., Thorson, J.S. & Soo, E.C. Selective detection of sugar phosphates by capillary electrophoresis/mass spectrometry and its application to an engineered *E. coli* host. *ChemBioChem* **8**, 1180–1188 (2007).